

## Using thermal spray coating method to produce system composites (Ni-Al<sub>2</sub>O<sub>3</sub>-B<sub>4</sub>C)

Amjad H.Jassim<sup>1</sup>, Salih Y. Darweesh<sup>2</sup>, Sufian H. Humeedi<sup>1</sup>

<sup>1</sup> Physics Department, College of Science, Tikrit University, Tikrit, Iraq

<sup>2</sup> Physics Department, College of Education TuzKhurmatu, Tikrit University, Tikrit

<https://doi.org/10.25130/tjps.v27i5.19>

### ARTICLE INFO.

#### Article history:

-Received: 6 / 7 / 2022

-Accepted: 28 / 7 / 2022

-Available online: / / 2022

**Keywords:** Mechanical Tests, Coating Porosity, Plasma Spraying, Cermet, Hardness, SEM.

#### Corresponding Author:

**Name:** Ibrahim K. Salman

E-mail:

[Amjad@tu.edu.iq](mailto:Amjad@tu.edu.iq)

[salih.younis@tu.edu.iq](mailto:salih.younis@tu.edu.iq)

[sufianhh@yahoo.com](mailto:sufianhh@yahoo.com)

**Tel:**

### ABSTRACT

Thermal plasma spraying method was used for coating the pre-prepared surfaces of turbine blades. Nickel (Ni) was used as a base material with a fixed percentage of alumina (5% Al<sub>2</sub>O<sub>3</sub>), and (5,10,15,20,25%) of Boron carbide (B<sub>4</sub>C) as reinforcement material. Cermet powders were mixed for one hour, then the coating bases of steel type (316L) were prepared and roughened using sandblasting to increase the adhesion strength between the coated materials and the base. The bonding material represented by (Ni-22% Cr-10% Al-1% Y) was sprayed with a thickness of (150 μm), and then the base and reinforcement material were sprayed with a thickness of (350-400 μm). Thus, the final thickness of the prepared samples was (550-500 μm). After that, the samples were sintered at 900°C for two hours. The hardness test was applied to the samples, indicating the best hardness after sintering at (25%) reinforcement ratio of 590Hv. As for porosity, its lowest value was obtained at 7%, while the best value of adhesion strength was obtained after sintering at (25%) of B<sub>4</sub>C. However, the results of the scanning electron microscope (SEM) showed the weakness and the presence of pores in the coating layers at the low percentage of reinforcement. While the mechanical and physical properties were improved with the increase in the percentage of reinforcement to reach the best at 25% of B<sub>4</sub>C.

### 1. Introduction

Thermal spraying with flame, particularly thermal spraying with plasma, is one of the most important techniques for treating damaged surfaces. In recent ten years, producing composite materials has witnessed high development in producing composite materials reinforced by fibers, powder, or peels, especially by casting, powder technology, or thermal spray coating. Thermal spray techniques have an advanced position in coating processes. It allows the use of a wide range of materials, from materials with low melting points to materials with high melting points and composites, to obtain good physical and mechanical properties of the coating. These techniques also generally considered the most widely used industrial means for external cladding for industrial requirements, especially for efficiently coating large pieces at high deposition rates. These techniques need high accuracy and control by the

coating coefficients and circumstances such as material feeding rate, air force, and the distance between the spray gun and the base to get coatings with good adhesive strength and high structural and mechanical properties [1-3]. The rehabilitation process and return of the turbine blade to the service again after processing and protecting the surfaces from cracks or crevices are necessary with great economic feasibility because of the high cost of blades and the engineering effort consequences of replacing the blades from the turbine engine[4]. Over the past few years, researchers made the first attempt to combine the data of these changes with different energy and thermal applications that provide good dielectric strength (thermal barrier coating) in the elevated temperature range, especially marine engines and gas turbines [5]. Depending on the matrix and cost, the temperature data is always affected by an

observation of less correlation than its own. The aliasing can have good mechanical properties to achieve an understandable imitation of the error. In addition to enhancing smoothness, the blended structure is designed as an alternative to traditional engineering materials such as alloys or polymers. As far as robust content is concerned, they have pushed themselves to stabilize non-standard content. This material can be a ceramic metal or a polymer. They come in different sizes and the powder can be fibrous or flaky [6]. Conformably, the different coating methods, including total plasma spraying, vigorous arc spraying, or spraying with high-speed oxygen fuel, etc., to protect surfaces from wear and crack [7].

**2. The Experimental Part**

**2.1. Materials**

The binder was a powder of (Ni-22 %, Cr- 10 %, Al- 1 % Y) produced at (Amdry 962) with a depth of (150 m) as well as a granular diameter (0.015 mm) of (-106 +53) μm. The reinforcement material (Ni) was manufactured by (Metco 480Ns) with a granular size (-90 +45) μm. As for the base material, it consisted of Boron carbide (B<sub>4</sub>C) and aluminum oxide (5% Al<sub>2</sub>O<sub>3</sub>) with thickness up to (550-450) μm and manufactured by (WISDOM) Company with a granular size (-45 +11) μm.

**2.2. Preparation Methods**

The cermet compound was made using (5 %) of Al<sub>2</sub>O<sub>3</sub>+Ni as a base material and Boron carbide (B<sub>4</sub>C) with different reinforcement percentages (5, 10, 15, 20, 25%). The particles were then thoroughly mixed for 2 hours using an electric mixer. The cermet composite powders were then subjected to a preliminary heat treatment at (100°C) for (30 minutes) prior to the coating process using an electric

oven with a heat thermostat manufactured in Germany. The produced coated bases were of (Stal Steel type 316L), after being flattened and trimmed to the proper sizes to fit inside the glass beaker. They were then cleaned in alcohol to get rid of the lubricant. To make the basic sample rougher, an Amit Tech grit blast tool was used. After sealant bases were roughened, they were prepared for spraying. Heat transfer plasma spraying (Thermal Spray Process) was applied using a device of (3MB collaborative innovation) of American origin to coat samples. The sand particles were used for hardening with a pressure of (5bar) and a radius variety from (70 percent mm to 1.6 mm). The spraying was used to create the electrochemical process that created plasma. The arcs were transferred between both the steel counter electrode and the metal anode electrodes, both of which were liquid. A mixture of primary gas made of helium or hydrogen was continuously injected further into arc, wherein flame was created as a result of mixture ionization. To generate higher temperatures at a shorter wavelength, supplementary gasses were employed to increase the arcs flame mixture's number of active sites or flame entropy (3000 °C). However, the work item received little or no heat, remaining comparatively cold. The spray parameters were designated by a sequence of tests to ensure that coatings with good adhesion strength and a certain thickness were obtained in order to determine the physical properties of the coating. A thermal treatment was also carried out for samples resulting from thermal spraying with plasma at a temperature of 900°C for only two hours. The parameters of spraying process are shown in table (1).

**Table 1: parameters of plasma spraying process**

Parameters	NiCrAlY	TiO <sub>2</sub> +Ni5Al
Type Gun	3MB METCO	3MB METCO
(SCFH)Argon drift rates	80	80
(SCFH) gas drift rate Hydrogen	15	15
Currents (A)	450	500
Voltages (V)	50	55
powder transporter Argon gas	30	30
Powder (Lbs./Hr.) feed rate	10	25
Spraying space	12	8

**3. Examinations and Tests**

**3.1. Spraying Angle**

The recommended angle for the flame thermal spraying technique is 90 degrees, yet the coating structure is unaffected even when the spraying angle is 45 degrees. The effect occurs when the angle is less than 45 degrees and has an impact on the coating's structure.

**3.2. Hardness Test**

After polishing and grinding coated samples both before and after thermal treatments, Vickers hardness was determined. The indentation was made using a diamond indenter with a pyramidal shape, a 136-degree angle between the opposing surfaces and a

100-gram load (10 sec). When the light indicator lit up, it was mechanically elevated when the allotted period of time had passed. The sizes of the imprint inside the three planes and in the two beams orientations were established by taking into consideration five measurements plus computing their algebraic means in order to calculate the impact toughness from the touchscreen that is placed on the item square. Vickers hardness is represented by the following equation [9]:

$$HV=1.854 \frac{P}{d_{av}^2} \text{ (Kg/mm}^2\text{) } \dots (1)$$

Where (HV) is Vickers hardness, (P) is the pressure applied in grams, and (d<sub>av</sub>) is the average indenter

diameter. Numerous sections of the sample were examined to see how hard they were. In order to determine a rough estimate of the hardness rate, the hardness of the center and the edges was calculated.

### 3.3. Porosity Test

One of the most crucial characteristics of thermal spray coating is the presence of pores. Knowing the values of the pores ratio in the coating is important since these pores have an impact on the coating's qualities. After removing the coating layer from the test matrix, in order to conduct the porosity test, fragments of the protective coating were used. In order to calculate the porosity ratio in compliance with standard specification no. (ASTM-C 830) [10]. The Archimedes principle (immersion method) was used which comprises the next steps:

Using a hearaeus electric furnace set at 75 °C to dry samples of the combined material for 30 minutes, followed by weighing the samples with a precise balance (0.0 01 mg). This weight is designated as ( $W_1$ ).

Submerging the samples in distilled water for two and a half hours, weighing the immersed samples, heating them to a temperature of 10°C, allowing them to cool, and then weighing them again. This weight is designated as ( $W_2$ ).

Weighing the samples while they are suspended in distilled water and submerged in it. This weight is known as ( $W_3$ ).

Determining the percentage of open pores ( $P_o$  %) using the following equation [11]:

$$p_o \% = \left[ \frac{W_2 - W_1}{W_2 - W_3} \right] \times 100 \dots (2)$$

### 3.4. Adhesion Test

According to the ASTM - (C 633) standard technical specification, the tension instrument, which had a load capacity of (1.5 Ton), continued to achieve adherence of the composite coating [10]. When carrying out the tests, the following procedures were followed:

Preparing the samples of matrix without coating in a number equal to the unsprayed samples by the same normal dimensions.

Using ethanol to chemically clean (treated and non-treated) specimens in order to get rid of contaminants that interfere with the connection of the two parts.

After approximately two hours of pressure, the two pieces were placed in a dry incubator for 24 hours at 50 °C.

Using epoxy to bind the pairs (unsprayed or sprayed), covering the whole coated area with a uniform, thin

layer of adhesives. Prior to the pressure test, constant adherence was essential. The force utilized to conduct the test must be totally perpendicular on the protective film.

Applying tensile loads to each test sample at a rate of one millimeter per minute until the sample with the highest load applied was identified and recorded. Calculating the stickiness and cohesion intensity of the covering on the carbon fiber using the following formula [11]:

$$\text{Adhesion Force} = \frac{F}{A} \dots (3)$$

Where: F: is force, A: area.

### 3.5. Scanning Electron Microscope Test

The particles required to run the microscope are generated by an electronic producer. There are also two spherical lens and an objective lens comparable to those found in microscopy. All parts are placed in a sealed container to avoid the influence of air molecules on protons. The specimen compartment, in which the particles are suspended for analysis, is on the opposite end. The bottom level of the facility is often where the lens is situated since it is vibration-insulated even though it is acutely susceptible to movement [12].

## 4. Results and Discussion

### 4.1. The effect of spraying angle on the porosity and hardness of the cermet coating

To investigate the impact of plasma spraying films' pores and roughness following thermal sintering of the prepared samples, different spraying angles (30°, 45°, 60°, 75°, and 90°) were chosen. Figure 1 demonstrates that the porosity was high at low angles (30°) and that not the coating's entire surface was covered by the stream of droplets colliding with it. As a result, a heterogeneous surface with a porous structure was formed with lower mechanical properties like hardness, resistance and adherence. However, when the spraying distance was raised above (4.5 m), the microstructure of the coating layers had an impact on the proportion of pores at the spraying angle, where a change in the spraying direction controlled how quickly the liquid aspect of creating flows, as shown in Fig. (2) on how the toughness of said cermet covering layer increased as a result of increasing spraying angles to (90°), which produced compact and homogeneous coating layers that were almost free of surface defects. All the molten drops filled the base surface at this angle perpendicular to it, generating a thick covering layer without surface flaws [14].

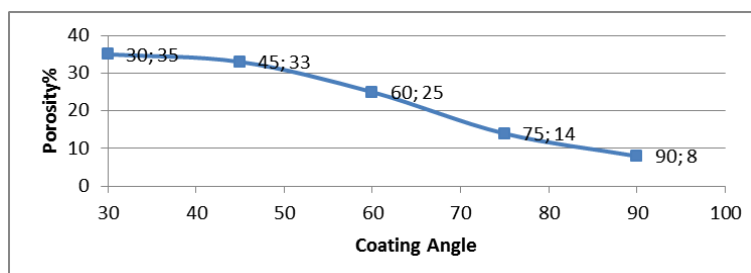


Fig. 1: Relationship of coating angle with porosity after sintering

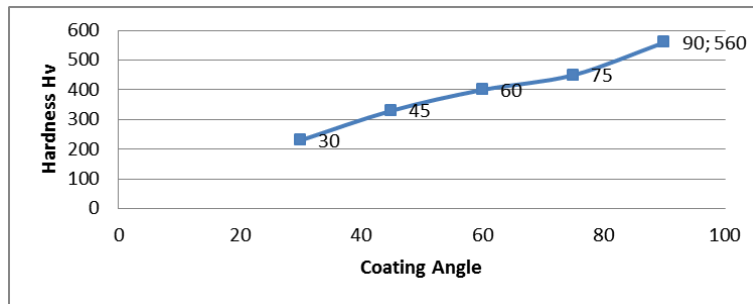


Fig. 2: Relationship of coating angle with hardness after sintering

4.2. The impact of reinforcing percentage on hardness value

The nutrient system's segments and hardness level before and after sintering are shown in Fig. 3 as a function of the metal reinforcement ratio. The hardness was low at low strengthening ratios due to the high porosity at these ratios, but as reinforcement ratios increased, the hardness increased as well. The hardness of the base, which was made of type 316L steel, was calculated when the porosity was as little as possible. Before the heat treatment, the hardness was (210Hv), and it was (460Hv) at (25 %) of B<sub>4</sub>C.

However, when the heat treatment was performed at (900°C) for only two hours, the hardness values increased and became higher and reached their highest value at (590Hv) with the same percentage above. This improved the hardness values due to the low percentage of pores as well as to the impact of nickel with such a high mechanical strength. This in turn improved the coated layer's characteristics because of sintering and diffusion processes that led to an increase in hardness values and physical characteristics of the system [15, 16].

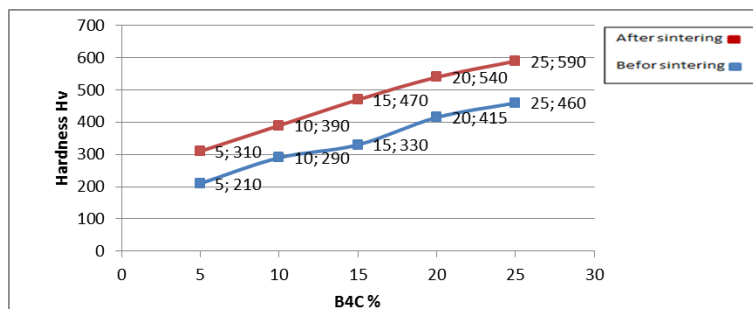


Fig. 3: The effect of reinforcement ratio on micro hardness before and after sintering

4.3. The Effect of reinforcement percentage on porosity

The porosity, one of the distinctive characteristics that allows for the strength and weakness of the cermet layer to be assessed by the ratios of the open pores during coating, was explored. The results can be understood from Figure (4), which shows the porosity before and after the heat treatment (sintering). It was revealed that using low ratios of reinforcement gives height porosity value for the coated layer and then gradually decreases through the addition of the carbide part (B<sub>4</sub>C), until it reaches a maximum porosity value of (25% of B<sub>4</sub>C), which showed the lowest porosity ratio (14%) prior to heat treatment. The high porosity may be attributed to the

molten droplets' inability to be completely flat and associated with other droplets due to the rapid cooling rate they experience during their propagation and as a result of the removal of heat from the basic. As a result, the droplets will experience thermal contraction after solidification [6, 14]. When it achieves the lowest percentage at (25% of B<sub>4</sub>C), which is (7 %), as shown in the same figure, then the percentage of porosity is less after the heat treatment of the ceramic coating layers than it was before. This indicates that because of the sintering rate, the movement of atoms between layers while attempting to seal the pores allows for the formation of new bonding areas between layers [15].

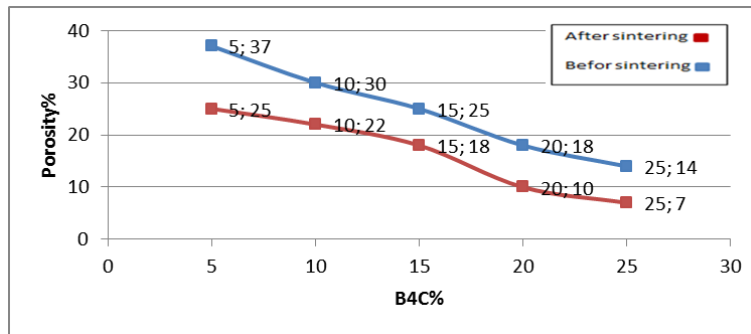


Fig. 4: The difference between reinforcement-induced porosity ratios before and after sintering

**4.4. The effect of reinforcement ratio on adhesion strength**

The adhesion force is bounding strength between the base surface and the cermet coating layer. The results of the examination of these models showed a value of (26 MPa) aimed at the adhesion forces at (25% of B<sub>4</sub>C) before the heat treatment, and the value of (38MPa) after the heat treatment on the samples for two hours at a temperature of ( 900°C) and at (25% of B<sub>4</sub>C). The best value of adhesion strength was found at the ratio (25% of B<sub>4</sub>C) of the Ni binder. As can be

seen from Figure 5, the adhesive force was low when the percentage of the binder was small, but it increased gradually as the amount of the binder did. This drop happened as a result of the binder's efforts to weaken the adhesive bond seen between coating material's atoms in favor of creating bonding regions between those atoms. The materials were produced by heating at 90 °C for two hours, which reduced the pores of the polymer film and improved the adhesives strength value. As a result, both hardness and the bonding strength were increased [16,17].

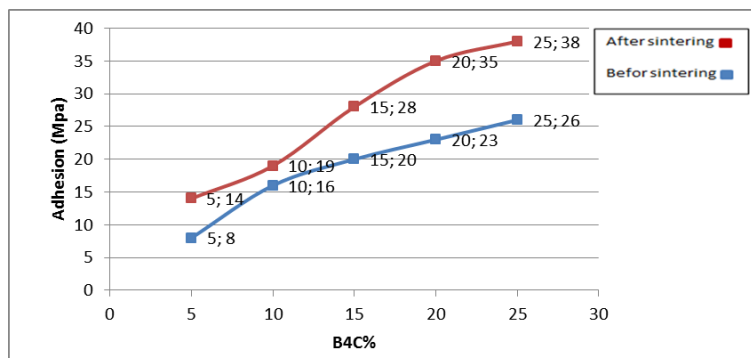


Fig. 5: Relationship between the adhesive strength and the additive's % before and after sintering.

**4.5. Compositional characteristics with varying reinforcement percentages by SEM**

Scanning electron microscope (SEM) was used to identify the most important features of the surface following the heat combustion method for such samples made using spraying technology. Images were collected at greater depths (m). The change in rates of adding carbide powder (% B<sub>4</sub>C) as a reinforcement material to the system (Ni-Al<sub>2</sub>O<sub>3</sub>) was studied. SEM image revealed that the nickel powder was dispersed and spread in a spherical shape, demonstrating that the powder used had a spherical shape, indicating the purity and homogeneity of the powder, assisting in achieving greater homogeneity with the reinforcement. Because the impurities work on creating interfaces during the plasma thermal spraying process, the samples lacked strength and the proportion of surface pores increased. Figure (6) shows samples that were sprayed and then heated at 900 °C for two hours of sintering. Figure 6(a) shows an image of a coating with reinforcement of (5% B<sub>4</sub>C). There was heterogeneity in the surface and the layer was weak in the coating because of the

insufficient bonding substance Ni, which increased the bonding of the oxide with the surface. In other words, when the temperature is high, the bonding substance is sufficient to create melting areas on regions of atoms and molecules of the base, which strengthens the adhesion [20]. As for figure (6-b), it shows the coating at reinforcement rate (10% B<sub>4</sub>C), where there were cracks in the coating's surface due to the absence of binding material, causing a lack of homogeneity. When increasing the reinforcement coating layer to (15 % B<sub>4</sub>C), as shown in figure 6-c, the coating layer improved and cracks nearly vanished. Figure (6-d) shows reinforcement rate (20 % B<sub>4</sub>C), where a homogeneous distribution of the compounds was discovered through the surface of the chromium oxide-alumina. This shift in the surface's perfection is prompted by the development of an interconnection area between the layers of coating. Ceramite attempts to close the pores when undergoing heat treatment as a result of the occurrence of sintering processes, diffusion of atoms through their transfer among themselves, and an increase in the binding material Ni. As for figure (6-



e), it provides a SEM image of the reinforcement material (25 %  $B_4C$ ), demonstrating a clear distribution of each of the substrate Ni- $Al_2O_3$  and the reinforcement  $B_4C$  %. As a result, almost all cracks and pores through the ceramic surface were vanished (75 % (Ni- $Al_2O_3$ ) -25 %  $B_4C$ ), indicating that the

surface shape became homogeneous and consistent with the binding material (dark Up until having the best value of the adhesion strength on the ratio (25 %) of the binder, the percentage of the binder will gradually increase [21, 22].

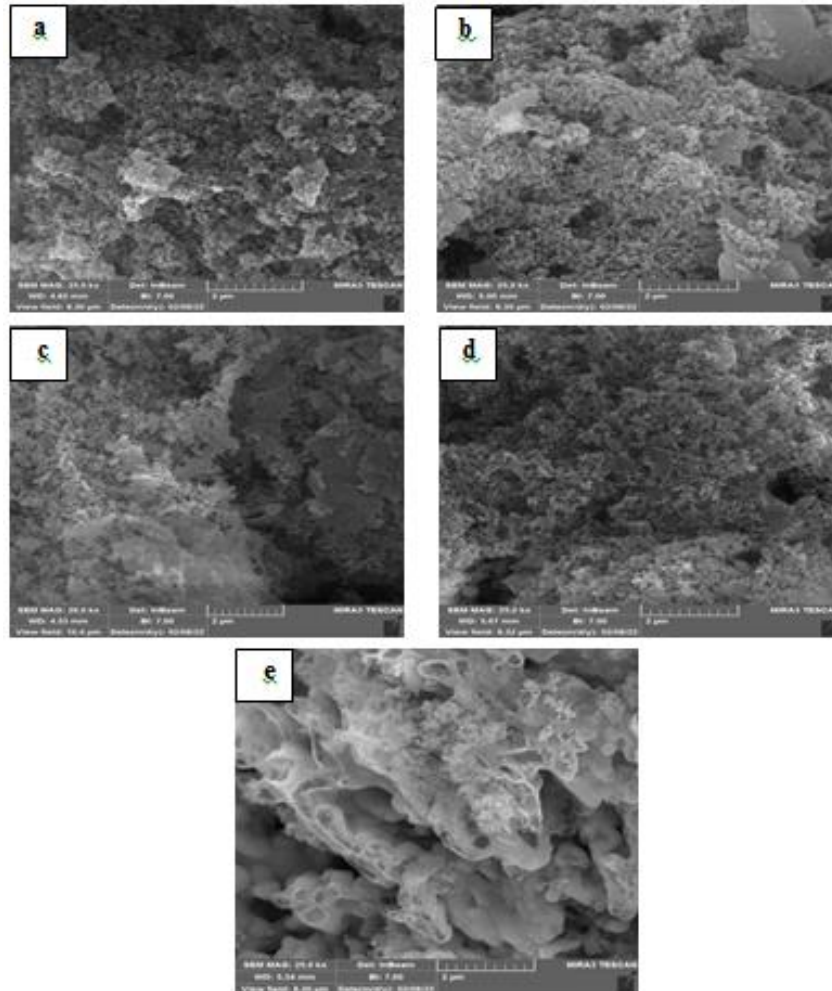


**Fig. 6: SEM images of the Cermet Composites (Ni-5% $Al_2O_3$ -% $B_4C$ ) Where: (a) 5%  $B_4C$ , (b) 10%  $B_4C$ , (c) 15%  $B_4C$ , (d) 20%  $B_4C$ , (e) 25%  $B_4C$**

### Conclusion

The paper in this study is applying thermal plasma spraying, it is possible to create a layer of cermet composite material with a base of Ni and alumina particles (5 %  $Al_2O_3$ ) supported by particles of  $B_4C$  as an adhesive compound on a foundation of an alloy of St.St. 316L. After coating and sintering for 2 hours at 900°C, adding more reinforced binder increases the

layer's adhesion degree between the base's surface. SEM results confirmed obvious consistency and tangling between its ceramic materials, showing a strong link between both the iron oxides and the nickel metals utilized as the bonding medium. The lack of flaws, specifically at (25%  $B_4C$ ), is evidence of the improvement in the composite material layer.

### References

- [1] Khalil, A. A., Tawfik, A., Hegazy, A. A., & El-Shahat, M. F. (2014). Effect of some waste additives on the physical and mechanical properties of gypsum plaster composites. *Construction and building materials*, 68, 580-586.
- [2] Lee, Donghwi, et al. "Enhanced flow boiling heat transfer on chromium coated zircaloy-4 using cold spray technique for accident tolerant fuel (ATF)

materials." *Applied Thermal Engineering* 185 2021: 116347.

- [3] Ceratti, D. R., Louis, B., Paquez, X., Faustini, M., & Grosso, D. (2015). A new dip coating method to obtain large-surface coatings with a minimum of solution. *Advanced Materials*, 27(34), 4958-4962.

- [4] Sarikaya, O. 2005. Effect of some parameters on microstructure and hardness of alumina coatings

prepared by the air plasma spraying process. *Surface and Coatings Technology*, 190(2-3), 388-393.

[5] Saha, M., & Mallik, M. (2021). Additive manufacturing of ceramics and cermets: present status and future perspectives. *Sādhanā*, 46(3), 1-35.

[6] Ahmed, H. H., Ahmed, A. R., Darweesh, S. Y., Khodair, Z. T., & Al-Jubbori, M. A. 2020. Processing of Turbine Blades Using Cermet Composite Materials. *Journal of Failure Analysis and Prevention*, 20(6), 2111-2118.

[7] Zhang, S., Han, B., Li, M., Zhang, Q., Hu, C., Jia, C., ... & Wang, Y. (2021). Microstructure and high temperature erosion behavior of laser cladded CoCrFeNiSi high entropy alloy coating. *Surface and Coatings Technology*, 417, 127218.

[8] Gerdeman, Dennis A., and Norman L. Hecht. "Arc plasma technology in materials science." 2012.

[9] Shahdad, Shakeel A., et al. "Hardness measured with traditional Vickers and Martens hardness methods." *Dental Materials* 23.9 2007: 1079-1085.

[10] Mohammed, S. F., & Darweesh, S. Y. 2018. Effect of Thermal Treatment on Some Physical and Mechanical Properties of Cermet Coating by Flame Spraying Technology. *Journal of University of Babylon for Pure and Applied Sciences*, 26(7), 269-280.

[11] Swain, B., et al. "Mechanical properties of NiTi plasma spray coating." *Journal of Thermal Spray Technology* 2020: 1-15.

[12] Kumar, R. (2021). Microscopy, working and types. *Asian Journal of Pharmacy and Technology*, 11(3), 245-248.

[13] Kumar, D., Shree, G., & Dwivedi, V. K. 2020. Wear and hardness evaluation of electrodeposited Ni-SiC nanocomposite coated copper. *International Journal of Microstructure and Materials Properties*, 15(2), 87-106.

[14] Habib, K. A., et al. "Influence of Al<sub>2</sub>O<sub>3</sub> particle size on microstructure, mechanical properties and

abrasive wear behavior of flame-sprayed and remitted NiCrBSi coatings." *Journal of Materials Engineering and Performance* 26.4 2017: 1647-1656.

[15] Riyadi, T. W. B. 2020. Structure and Properties of Ni- Al- Ti Systems Formed by Combustion Synthesis. In *Materials Science Forum* (Vol. 991, pp. 44-50). Trans Tech Publications Ltd.

[16] Darweesh, S. Y. 2014. Study of physical properties of Cermet coating layers (Al<sub>2</sub>O<sub>3</sub>+ ZrO<sub>2</sub>+ Ni-Al) prepared by flame thermal spray technology. Master Physics, University of Tikrit, Collage of Education for Pure science, 30.

[17] Pugazhendhi, A., Vasantharaj, S., Sathiyavimal, S., Raja, R. K., Karuppusamy, I., Narayanan, M., ... & Brindhadevi, K. (2021). Organic and inorganic nanomaterial coatings for the prevention of microbial growth and infections on biotic and abiotic surfaces. *Surface and Coatings Technology*, 425, 127739.

[18] Ozgurluk, Y. (2022). Investigation of oxidation and hot corrosion behavior of molybdenum coatings produced by high-velocity oxy-fuel coating method. *Surface and Coatings Technology*, 128641.

[19] Bolelli, Giovanni, et al. "TiC-NiCr thermal spray coatings as an alternative to WC-CoCr and Cr<sub>3</sub>C<sub>2</sub>-NiCr." *Wear* 450, 2020: 203273.

[20] Dahham, A.T., Humeedi, S.H., Darweesh, S.Y., Khodair, Z.T.," The Effect of Adding Nickel Content to Turbine Blades Coating Using Thermal Flame Spraying", *Scientific Journal of King Faisal University*, 2020, 21(2), pp. 29-34.

[21] Zeynelabdien, H. A., Mahmood, A. S., & Majeed, Z. N. (2021, September). Effect of Addition of Tungsten Carbide on the Structural and Physical Properties of an Aluminum-Based System By Powder Method. In *Journal of Physics: Conference Series* (Vol. 1999, No. 1, p. 012065). IOP Publishing.

استخدام طريقة الطلاء بالرش الحراري لإنتاج متراكبات بنظام (Ni-Al<sub>2</sub>O<sub>3</sub> \_B<sub>4</sub>C)أمجد حسين جاسم<sup>1</sup> , صالح يونس درويش<sup>2</sup> , سفيان حواس حميدي<sup>1</sup><sup>1</sup> قسم الفيزياء ، كلية العلوم ، جامعة تكريت ، تكريت ، العراق<sup>2</sup> قسم الفيزياء ، كلية التربية طوزخرماتو ، جامعة تكريت ، تكريت ، العراق

## الملخص

تعد طريقة الرش بالبلازما الحرارية المستخدمة لغرض طلاء الأسطح المحضرة مسبقاً للرش التوربينات ، حيث تم استخدام النيكل (Ni) كمادة أساسية مع نسبة ثابتة من الألومينا 5% Al<sub>2</sub>O<sub>3</sub> ، وتم تقوية القاعدة بكمية البورون B<sub>4</sub>C . بنسب (5،10،15،20،25)% حيث تم خلط مساحيق السيراميكية لمدة ساعة ثم تحضير قواعد الطلاء والتي كانت من النوع الفولاذي (316) وتم تخشينها باستخدام القصف الرملي لزيادة قوة التصاق بين المواد المطلية والقاعدة. تم رش مادة الترابط الممثلة بـ Ni-22% ، Cr-10% ، Al-1% (Y بسمك (150 ميكرومتر) ثم رش المادة القاعدية والمقواة بسمك (350-400 ميكرومتر) بحيث أن السماكة النهائية للعينات المحضرة كانت (550-500 ميكرومتر). لبدت العينات المأخوذة من الرش عند 900 درجة مئوية لمدة ساعتين، وتم إجراء اختبار الصلابة عليها ، والذي أعطى أفضل صلابة للعينات بعد التليد بنسبة تقوية 25% عند 590 Hv، بينما أقل قيمة للمسامية. وبالنسبة لأعلى نسبة تم الحصول عليها أيضاً عند 7% ، بينما كانت قوة الالتصاق بعد التليد عند 25% B<sub>4</sub>C هي (38 ميغا باسكال)، لكن نتائج الفحص بالمجهر الإلكتروني (SEM) أظهرت وجود ضعف وظهور المسام في طبقات الطلاء عند نسبة منخفضة من التدعيم، بينما تحسنت الخواص الميكانيكية والفيزيائية بزيادة نسبة التدعيم لتصل إلى الأفضل عند 25% B<sub>4</sub>C.